



Prediction of Favorite Positions of Fluoride Atoms Doped in Strontium Manganite using Atomistic Simulation

Abdalla Abdelrahman Mohamed
E-mail: abdallam194@gmail.com

Abstract

A set of interatomic potentials has been derived for the determination of the most favorable sites of the oxygen substituted by fluorine atoms in SrMnO_3 . The calculations were performed using GULP code which implements interatomic potentials calculations within the ionic shell model. Initial investigations were made on SrMnO_3 perovskite material. Our results for the parent SrMnO_3 are in agreement with experimental data. This substitution is favorable to full Schottky disorder and the fluorine atoms are predicted to occupy sites *trans* to each other in the octahedron surrounding Mn.

Keywords: Prediction, Doping, Atomistic, Simulation, Perovskite, Gulp

1. Introduction

Transition metal oxides form a large class of compounds that show intriguing and often technologically useful electronic and magnetic properties. Moreover, they are simple to manipulate experimentally and their early study allows them to provide test systems for new methods. By structural and compositional tuning, such compounds can exhibit a large variety of interesting properties. . Recently, a number of

transition-metal doped semiconductors [for example (Ruf et al. 2016). (Yuan, Du, and Xu 2016). (Strelchuk et al. 2016). (Stoica and Lo 2014a). (Pazhanivelu et al. 2016)] and doped mixed oxides [for example (Bettaibi et al. 2016). (Muralidharan et al. 2016). (Alippi, Cesaria, and Fiorentini 2014). (Stoica and Lo 2014b)] have been identified often as thin films. However these materials used metals as dopants. We suggest here that such

materials can be produced via anion-doping such as fluorine ions. But the researchers were unable to distinguish whether the fluoride ions occupied the Cis or Trans sites. Doped fluorine in strontium manganite by insertion or replacement of oxygen have become a useful chemical way for Alternating the valence of transition metal which in turns lead to a profound modification of electric and magnetic properties. The goal of these investigations is to determine the favorite sites of the F dopant in the crystal structure of SrMnO₃ perovskite.

2. Computational Method

The computational simulation technique used is based upon the well establish program General Utility Lattice Program GULP (Gale 1997). All calculations are based upon the Born model of ionic solid (Born and Landé 1918) with ions assigned integral charges corresponding to their formal oxidation state (Mayer 1933). The interactions between the ions are formulated in term of short range forces that account for electron cloud overlap, long range columbic forces and dispersion Vander Waals interactions. The short range interactions are modeled with a Buckingham potential

$$E_{\text{Latt}} = \frac{1}{4\pi\epsilon_0} \sum_{i \neq j} \frac{q_i q_j}{r_{ij}} + A e^{-\frac{r_{ij}}{\rho}} - \frac{C}{r_{ij}^6} \quad (1)$$

Where A_{ij} , ρ_{ij} and C_{ij} are the adjustable parameters, r_{ij} are the interionic separation and q_i and q_j are the charges on ions i and j respectively. The parameters of the short-range potential were derived using a multi-structure-fitting procedure, described elsewhere (Agulló-López, Catlow, and Townsend 1988). (Minervini, Grimes, and Sickafus 2000) and are reported in Table 2. Equation (1) represents the lattice energy of the parent compound.

The calculation of defect formation energy utilized the Mott-Littleton approach (Mott and Littleton 1938) in which the crystal surrounding the defect divided into three regions. In the first region all ions are exactly using the Interatomic potentials and allowed to relax their positions in response to the defect. In the two outer regions the calculation of the displacement of the ions is approximated by assuming a dielectric continuum response to the electrostatic force of the defect (Harding 1990). In the first outer region, the displacement of individual ions are considered in calculation of the defect energy, whereas in the outermost the

forces due to the defect are relatively weak, and only polarization of sub-lattice is considered. In the calculations quoted here radii of the first and second region were set at 7 and 15 Å respectively.

3. Results and Discussion

3.1. Perfect Lattice

All calculations are done on an ordinary personal computer. Before carrying out defect calculations, and in order to further justify the model employed here, the perfect unit cell was relaxed to zero strain using energy minimization at constant pressure. The experimental unit cell dimensions and ion position of cubic SrMnO₃ structure of phase (*pm* $\bar{3}$ *m*), a=3.80(2) Å were optimized at 0 K condition using 1x1x1 cell. Our optimized structure is in a good agreement with the experimental results (Takeda and Ohara 1974). The atoms coordinate's positions are given in table1. The Buckingham interatomic potentials taken from GULP libraries (Wolskaa et al. 2000). (Binks 1994). (Lewis and Catlow 1986). [8] and [9, 10, 11] are given in table 2. Our optimized lattice constant is a=3.808 Å.

Table 1: The coordinates of the asymmetric unit cell of SrMnO₃

Ions	a-axis	b-axis	c-axis
Sr	0.5	0.5	0.5
Mn	0.0	0.0	0.0
O1	0.5	0.0	0.0
O2	0.0	0.5	0.0
O3	0.0	0.0	0.5

3.2. Intrinsic defect processes

There are eight unique intrinsic defect species found in strontium manganese oxides, these are the: $V_{O1}^{\bullet\bullet}$, $V_{O2}^{\bullet\bullet}$, $V_{O3}^{\bullet\bullet}$, $V_{Mn}^{////}$, $V_{Sr}^{//}$, $O_i^{//}$, $Mn_i^{\bullet\bullet\bullet\bullet}$, $Sr_i^{\bullet\bullet}$, all of which can be formed by one of the Schottky or Frenkel disorder processes. Table3 shows defect energies for a range of possible individual defects in SrMnO₃.

It has been demonstrated that Schottky defect formation is the dominant mechanism of intrinsic ionic disorder in perovskites (Lewis and Catlow 1986). (Akhtar et al. 1995) [12, 13] owing to the close-packed nature of the structure. The full Schottky can be written using Kröger-Vink notation (Kröger and Vink 1956). (Kroger 1974) as:

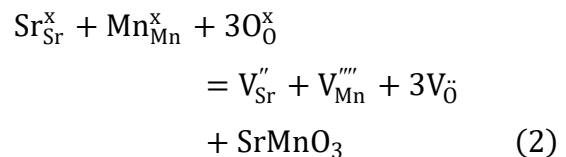


Table 2: Interatomic Buckingham potentials for SrMnO₃.

Interactions	A (eV)	ρ (Å)	C (eV×Å ⁶)
Sr ²⁺ shel O ²⁻ shel	1956.702	0.3252	0.00
Mn ⁴⁺ core O ²⁻ shel	3329.388	0.2642	0.00
O ²⁻ shel O ²⁻ shel	25.410	0.6937	32.32

Table 3: Individual defect energies.

Defect	Defect energy (eV)
V _{O1}	17.31670973
V _{O2}	17.31676043
V _{O3}	17.31676043
V _{Mn} ^{///}	97.21017776
V _{Sr} ^{//}	21.53345002
O ₁ ^{//}	-4.85332335
Mn _i ^{'''}	-72.2226508
Sr _i ^{''}	-2.67479465

with the associated defect reaction energy defined with respect to isolated ion removal and the addition of one formula unit to the bulk lattice ($E[\text{SrMnO}_3]$):

$$E_{\text{Schottky}} = \frac{1}{5} (E[V_{\text{Sr}}''] + E[V_{\text{Mn}}'''] + E[V_{\text{O}}^{\bullet\bullet}] + E[\text{SrMnO}_3]) \quad (3)$$

Owing to the high energetic cost of creating a highly charged Mn vacancy, partial Schottky formation in the SrO sub-lattice can become a competitive process:



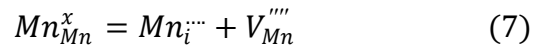
where the defect reaction is defined with respect to the standard state of SrO:

$$E_{\text{Schottky}}^{\text{partial}} = \frac{1}{2} (E[V_{\text{Sr}}''] + E[V_{\text{O}}^{\bullet\bullet}] + E[\text{SrO}]) \quad (5)$$

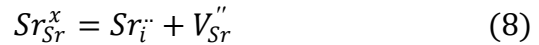
Oxygen Frenkel defect:



Manganese Frenkel defect:



SrO Frenkel defect:



The lattice energy for each compound was calculated according to equation (1), for SrMnO₃ is -159.3293 eV, and for SrO is -33.3419 eV.

The formation energies for full and partial Schottky defects, as well as the component elementary defects, are shown in table 4.

Table 4: Calculated energies of intrinsic atomic defects in SrMnO₃

Schottky and Frenkel Defects [eV/defect]		
Reaction	Equation No.	energy [eV per defect]
Full Schottky	2	2.2730
SrO Schottky	4	2.7542
O Frenkel	5	6.2318
Mn Frenkel	6	12.4938
Sr Frenkel	7	9.4294

One main point can be made of table 4, in SrMnO₃ perovskite, the O Frenkel, Mn Frenkel, Sr Frenkel and SrO Schottky disorders are unfavorable to occur, and the full Schottky defect reaction is the dominant (lowest energy) process, and is the most probable intrinsic disorder.

3.3. Fitting interatomic parameters

Before we do any defect calculations, we need to know some more interatomic potential which can help to complete our defect calculations correctly. There are two approaches to do so; first approach is to search these interatomic potentials in the potentials libraries provided by the GULP. If there are not such potentials in the GULP libraries, this is our case; we have to apply the second approach. The second approach is to use semiempirical data to fit the potentials we need. To be able to do defects calculation we need to find computationally the interatomic potential for Sr²⁺-F¹⁻, Mn⁴⁺-F¹⁻ and Mn³⁺-F¹⁻, while we found O²⁻-F¹⁻ and F¹⁻-F¹⁻ in interatomic potentials libraries. These have been done with interatomic pair potentials developed with the aid of a fitting procedure using elastic constants of the pair elements. Table 5 and table 6 gives the fitting parameters.

There are the only two ways we can substitute 2 F¹⁻ atoms for 2 O²⁻, *cis* substitution or *trans* substitution. The defect calculations will tell us whether 2F substituted *trans* are more or less favorable than 2F substituted *cis*, thereafter we can use these results as input for ab initio calculations.

Trans mean that the angle between two Mn atoms in the cell is 180°, and *cis* means that the angle between two Mn atoms is 90° as shown in the Figure below.

Computationally To distinguish *cis* substitution from *trans*, we need to replace two O by F. For *trans* we ran bulk defect calculations on replace O at 0.5, 0.0, 0.0 and -0.5, 0.0, 0.0 by F (*trans*), and another run for replace O at 0.5, 0.0, 0.0 and 0.0, 0.5, 0.0 by F (*cis*).

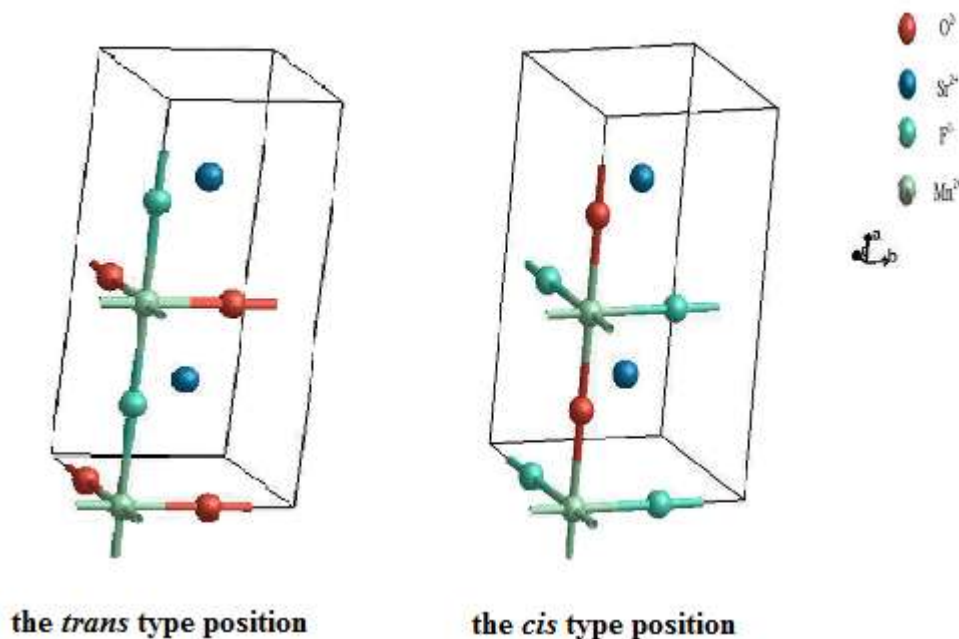
Table 5: Fitted potential parameters for SrMnO₂F

Interactions	A (eV)	ρ(Å)	C (eV×Å ⁶)
Sr ²⁺ shel F ¹⁻ shel	2193.899	0.298	0.000
Mn ⁴⁺ core F ¹⁻ shel	305.664	0.472	0.472
Mn ³⁺ core F ¹⁻ shel	252.495	0.436	0.000

Table 6: Shell model parameters Y and k refer to the shell charge and harmonic spring constant respectively.

species	Y/e	K/ev Å ⁻²
Mn ⁴⁺	4	95
Mn ³⁺	3	95
O ²⁻	-2.513	20.53
Sr ²⁺	1.831	71.7
F ⁻	-1.339	38

The other way is Replacing O by F (*cis*). Our optimized calculations revealed that the lattice energy is -114.30528 eV and lattice parameters a= 8.285218 Å, b= 4.520370 Å and c= 4.520370 Å with angles $\alpha=\beta=\gamma=90^\circ$, which means that we predict to have a tetragonal crystal structure of this compound. As the *trans* type position of replacing O by F has the lower lattice energy than the *cis* type, the fluorine atoms are



Due to the use of supercell 1x1x2 in these calculations, we used Cartesian coordinates instead of fractional. In replacing O by F (*trans*) our optimized calculations revealed that the lattice energy is -199.06334 eV and lattice parameters a=8.8575 Å, b= 3.9524 Å and c=3.9524 Å with angles $\alpha=\beta=\gamma=90^\circ$.

predicted to occupy sites *trans* to each other in the octahedron surrounding Mn.

4. Conclusion

Gulp calculations on models of SrMnO₂F suggested that the optimized parent

compound structure is not only in agreement with the experimental data but very close to it which means that our starting point of these simulations is a good start. The doping of fluorine atoms into the parent compound SrMnO₃ suggested that the F¹⁻ substitutes for O²⁻ creating change in the oxidation state of some manganese atoms. This substitution is favorable to full Schottky disorder, and the *trans* substitution of Fluorine atoms is more favorable than *cis* substitution.

References

- Agulló-López, Fernando, Charles Richard Arthur Catlow, and Peter David Townsend. 1988. *Point Defects in Materials*. Academic press.
- Akhtar, M. Javed, Zeb-Un-Nisa Akhtar, Robert A. Jackson, and C. Richard A. Catlow. 1995. "Computer Simulation Studies of Strontium Titanate." *Journal of the American Ceramic Society* 78 (2): 421–428.
- Alippi, Paola, Maura Cesaria, and Vincenzo Fiorentini. 2014. "Impurity-Vacancy Complexes and Ferromagnetism in Doped Sesquioxides." *Physical Review B* 89 (13): 134423.
- Bettaibi, A., R. M'nassri, A. Selmi, H. Rahmouni, K. Khirouni, N. Chniba Boudjada, and A. Cheikhrouhou. 2016. "Effect of Small Quantity of Chromium on the Electrical, Magnetic and Magnetocaloric Properties of Pr 0.7 Ca 0.3 Mn 0.98 Cr 0.02 O 3 Manganite." *Applied Physics A* 122 (3): 232.
- Binks, D. J. 1994. *Computational Modelling of Zinc Oxide and Related Oxide Ceramics PhD University of Surrey*. Harwell.
- Born, M., and A. Landé. 1918. "Verhandl. Deut. Physik." *Ges* 20: 210.
- Gale, Julian D. 1997. "GULP: A Computer Program for the Symmetry-Adapted Simulation of Solids." *Journal of the Chemical Society, Faraday Transactions* 93 (4): 629–637.
- Harding, J. H. 1990. "Computer Simulation of Defects in Ionic Solids." *Reports on Progress in Physics* 53 (11): 1403.
- Kröger, F. A., and H. J. Vink. 1956. "Solid State Physics, Vol. 3." *Edited by F. Seitz and D. Turnbull Academic Press, New York*, 307.
- Kroger, Ferdinand Anne. 1974. "The Chemistry of Imperfect Crystals." *Amsterdam. Netherlands* 2.
- Lewis, G. V., and C. R. A. Catlow. 1986. "Defect Studies of Doped and Undoped Barium Titanate Using Computer Simulation Techniques." *Journal of Physics and Chemistry of Solids* 47 (1): 89–97.
- Mayer, Joseph E. 1933. "Dispersion and Polarizability and the van Der Waals Potential in the Alkali Halides." *The Journal of Chemical Physics* 1 (4): 270–279.
- Minervini, Licia, Robin W. Grimes, and Kurt E. Sickafus. 2000. "Disorder in Pyrochlore Oxides." *Journal of the American Ceramic Society* 83 (8): 1873–1878.
- Mott, N. F., and M. J. Littleton. 1938. "Conduction in Polar Crystals. I. Electrolytic Conduction in Solid Salts." *Transactions of the Faraday Society* 34: 485–499.
- Muralidharan, M., V. Anbarasu, A. Elaya Perumal, and K. Sivakumar. 2016. "Enhanced Ferromagnetism in Cr Doped SrMoO₄ Scheelite Structured Compounds." *Journal of Materials Science: Materials in Electronics* 27 (3): 2545–2556.

- Pazhanivelu, V., A. Paul Blessington Selvadurai, Yongsheng Zhao, R. Thiyagarajan, and R. Murugaraj. 2016. "Room Temperature Ferromagnetism in Mn Doped ZnO: Co Nanoparticles by Co-Precipitation Method." *Physica B: Condensed Matter* 481: 91–96.
- Ruf, Thomas, Sergej Repp, Joanna Urban, Ralf Thomann, and Emre Erdem. 2016. "Competing Effects between Intrinsic and Extrinsic Defects in Pure and Mn-Doped ZnO Nanocrystals." *Journal of Nanoparticle Research* 18 (5): 109.
- Stoica, Maria, and Cynthia S. Lo. 2014a. "P-Type Zinc Oxide Spinels: Application to Transparent Conductors and Spintronics." *New Journal of Physics* 16 (5): 055011.
- . 2014b. "P-Type Zinc Oxide Spinels: Application to Transparent Conductors and Spintronics." *New Journal of Physics* 16 (5): 055011.
- Strelchuk, V. V., A. S. Nikolenko, O. F. Kolomys, S. V. Rarata, K. A. Avramenko, P. M. Lytvyn, P. Tronc, Chan Oeurn Chey, Omer Nur, and Magnus Willander. 2016. "Optical and Structural Properties of Mn-Doped ZnO Nanorods Grown by Aqueous Chemical Growth for Spintronic Applications." *Thin Solid Films* 601: 22–27.
- Takeda, Takayoshi, and Soji Ohara. 1974. "Magnetic Structure of the Cubic Perovskite Type SrMnO₃." *Journal of the Physical Society of Japan* 37 (1): 275–275.
- Wolskaa, E., J. Darula, W. Nowickia, P. Piszoraa, M. Tovarb, O. Prokhnenkob, C. Bahtzc, and M. Knappc. 2000. "X-Ray and Neutron Diffraction Studies on Cation Distribution in the LiMn₂O₄/LiFe₅O₈ Spinel Solid Solutions." *J. Solid State Chem* 153: 310.
- Yuan, Huan, Xiaosong Du, and Ming Xu. 2016. "Ferromagnetic Mechanism of (Co, Cu)-Codoped ZnO Films with Different Co Concentrations Investigated by X-Ray Photoelectron Spectroscopy." *Physica E: Low-Dimensional Systems and Nanostructures* 79: 119–126.